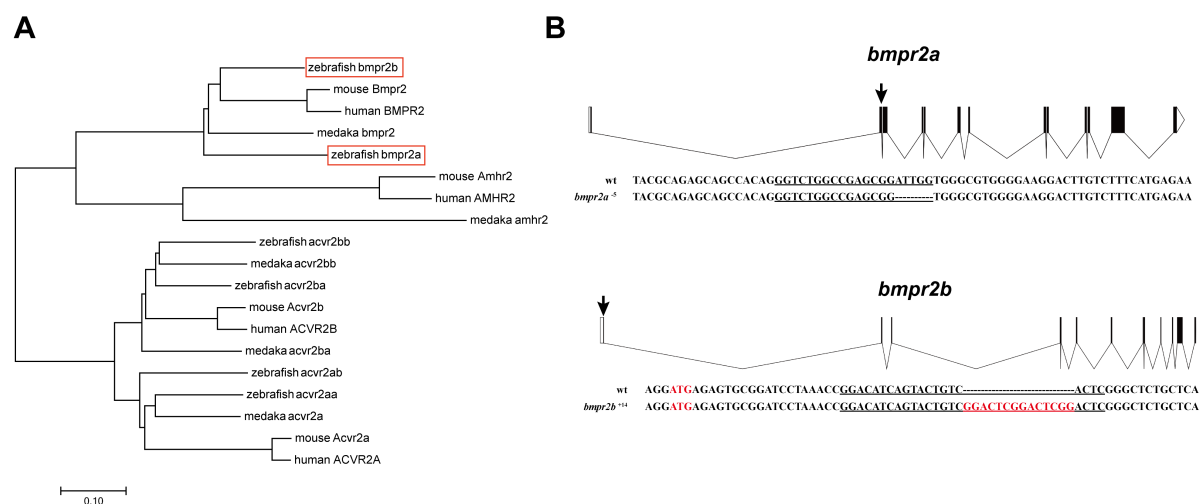


Supplemental Figures and Tables

**Fig. S1. Bmpr2 receptors (*bmpr2a* and *bmpr2b*) in zebrafish**

(A) Phylogenetic analysis of zebrafish *bmpr2a* and *bmpr2b*. The sequences were obtained from Genbank and Ensemble databases. Sequence alignment and tree construction were performed by MEGA software using Neighbor-Joining method. (B) Schematic illustration of CRISPR targeting sites of *bmpr2a* and *bmpr2b* in zebrafish. The arrows indicate the location of targeting sites. Open and solid boxes indicate untranslated and coding exons respectively. Sequences underlined indicate the CRISPR targeting sites and the underlined sequences in red are inserted bases.

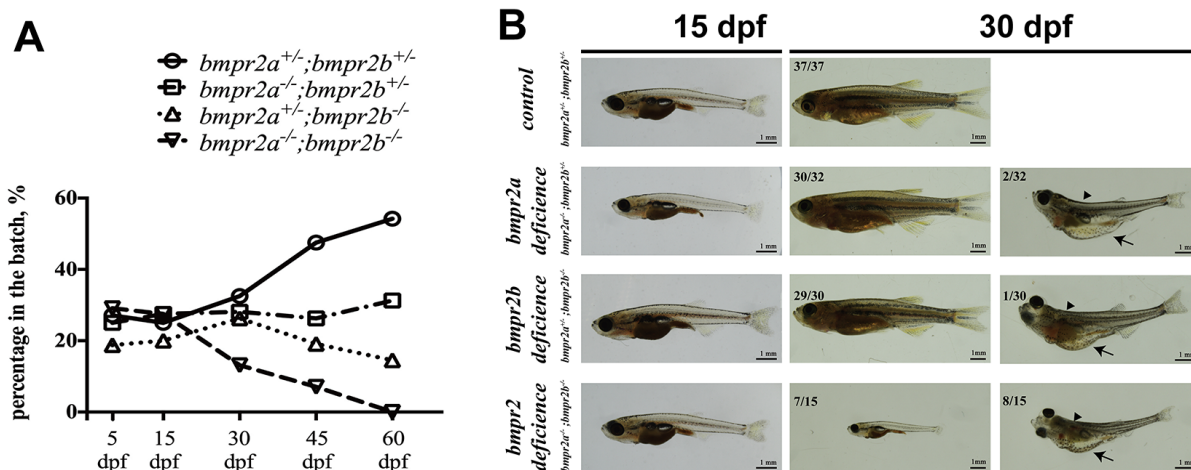


Fig. S2. *Bmpr2* deficiency leads to severe developmental defects

The female $bmpr2a^{-/-};bmpr2b^{+/-}$ was crossed with male $bmpr2a^{+/-};bmpr2b^{-/-}$ to produce the offspring with theoretical ratios 1:1:1:1 for different genotypes. The offspring were sampled at different time points (5-60 dpf) for genotyping (A). No obvious abnormalities were observed before 15 dpf among the four genotypes: wild type control ($bmpr2a^{+/-};bmpr2b^{+/-}$), single mutants ($bmpr2a^{-/-};bmpr2b^{+/-}$ and $bmpr2a^{+/-};bmpr2b^{-/-}$) and double mutant ($bmpr2a^{-/-};bmpr2b^{-/-}$) in terms of survival rate, morphology and growth. However, a significant mortality was observed in the $bmpr2$ -deficient double mutant at 30 dpf. The double mutant individuals ($bmpr2a^{-/-};bmpr2b^{-/-}$) that survived at this age all showed obvious developmental defects including edematous abdominal cavity (8 out of 15) and retarded body growth with much smaller body size (7/15) (B). From 30 to 60 dpf, the ratio of double mutant continued to decrease progressively; however, the ratios of the wild type and single mutants did not increase proportionally with the wild type steadily increasing while the single mutants remaining relative constant.

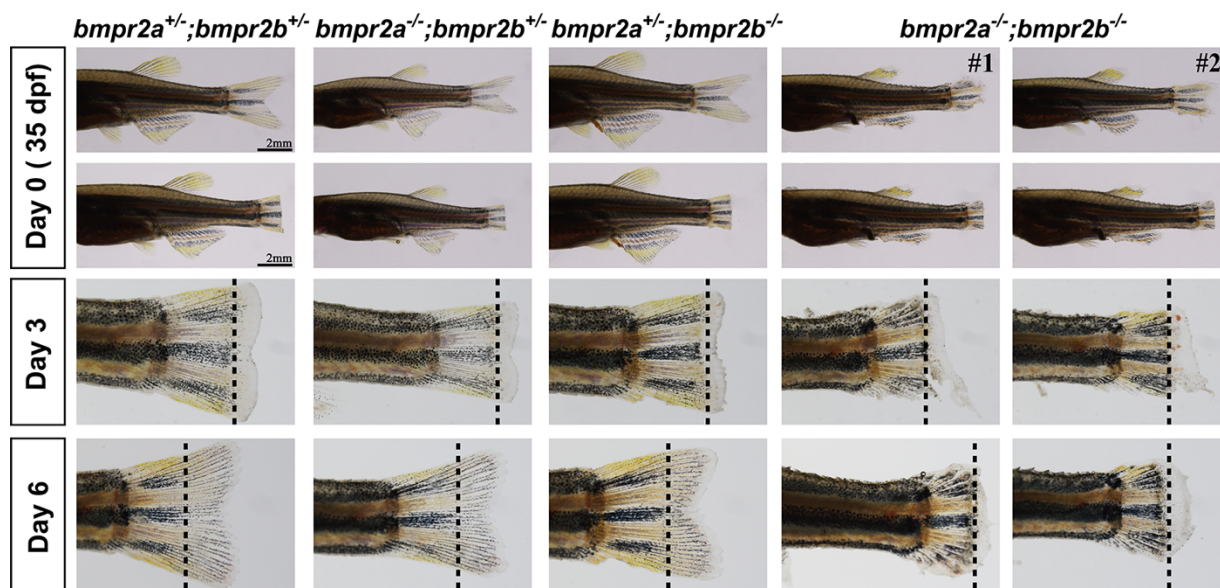


Fig. S3. Defective fin regeneration due to *bmpr2* deficiency

In addition to abdominal edema and retarded growth, some survived double mutants showed abnormal morphology of caudal fin at 35 dpf. To further confirm the role of *bmpr2* signaling in fin development, we performed a caudal fin regeneration assay by amputating the caudal fins at 35 dpf. The dotted line indicates the initial amputation plane. The double mutants (*bmpr2a^{-/-};bmpr2b^{-/-}*) displayed a quick regeneration with epidermal outgrowth beyond the amputation plane, similar to the single mutants (*bmpr2a^{-/-};bmpr2b^{+/-}* and *bmpr2a^{+/-};bmpr2b^{-/-}*) and control (*bmpr2a^{+/-};bmpr2b^{+/-}*) at 3 days post amputation (dpa). At 6 dpa, the control and single mutants had fully regenerated the caudal fins with fin rays well developed and tail fork well formed; in contrast, the regeneration of the caudal fins in the double mutants remained unchanged as compared to that at 3 dpa and the regenerated region was covered by the epidermis only without fin rays. The data suggested that *bmpr2* signaling was essential for maintaining normal fin morphology and promoting fin regeneration, and that *Bmpr2a* and *Bmpr2b* could functionally compensate for each other in this regard.

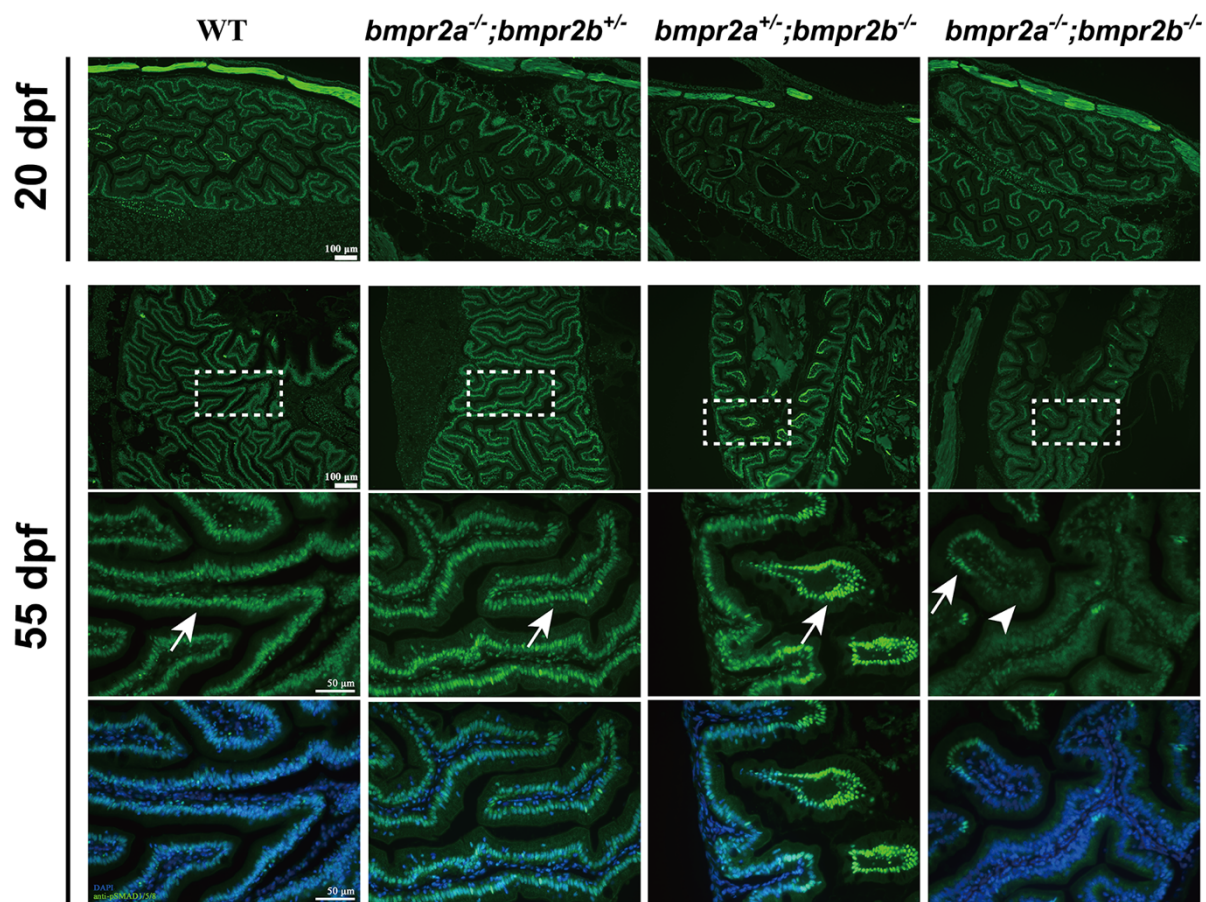


Fig. S4. *Bmpr2* deficiency reduces Smad1/5/8 phosphorylation in the intestine

To demonstrate whether the *bmpr2a* and/or *bmpr2b* mutation disrupts BMP signaling activity, we examined the phosphorylation of Smad1/5/8 by immunofluorescent staining for the signal of phosphor-Smad1/5/8 (pSmad1/5/8). At 20 dpf, a strong pSmad1/5/8 signal was observed in the intestines of all genotypes including control (WT), *bmpr2a* and *bmpr2b* single mutants (*bmpr2a*^{-/-};*bmpr2b*^{+/-} and *bmpr2a*^{+/-};*bmpr2b*^{-/-}), and the *bmpr2a*-deficient double mutant (*bmpr2a*^{-/-};*bmpr2b*^{-/-}). At 55 dpf, the pSmad1/5/8 signal remained strong in the intestinal epithelial cells in control and single mutants (arrows); however, the signal was absent in most of the epithelium cells of the *bmpr2*-deficient double mutants (arrowhead). Interestingly, this was the time window when most double mutants died.

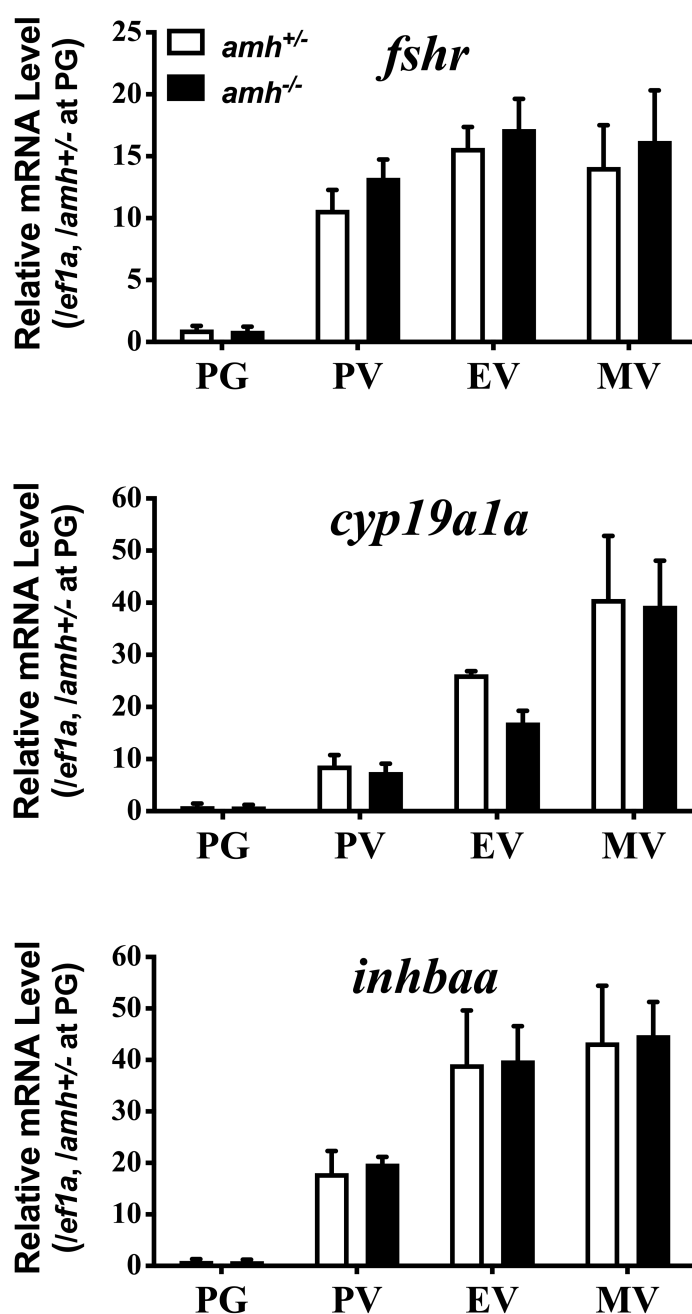


Fig. S5. Expression of *fshr* (FSH receptor), *cyp19a1a* (ovarian aromatase) and *inhbaa* (activin β A) in follicles of *amh* mutant

Follicles of PG (primary growth), PV (pre-vitellogenic), EV (early vitellogenic) and MV (mid-vitellogenic) were isolated from *amh* mutant ($amh^{-/-}$) and control fish ($amh^{+/-}$) for RNA extraction and qPCR quantification. The expression level of each target gene was normalized to the housekeeping gene *efl1a* in the same sample and expressed as the ratio to that of control PG ($amh^{+/-}$). The values are mean \pm SEM (n = 3). No significant difference was observed between *amh* mutant and control at any stage examined.

Table S1. Primers used

Gene name	Primer name	Primer sequence (5' to 3')	Application	
<i>bmpr2a</i>	bmpr2a-3301	TAGGTCTGGCCGAGCGGATTGG	sgRNA	
	bmpr2a-3302	AAACCCAATCCGCTCGGCCAGA		
<i>bmpr2b</i>	bmpr2b-3345	TAGGACATCAGTACTGTCACTC		
	bmpr2b-3346	AAACGAGTGACAGTACTGATGT		
<i>amh</i>	amh_2039	AGGCAAGATTTGGGCTGATG	HRMA	
	amh_2040	CTTCGGGTTGTTGTCCTGC		
<i>bmpr2a</i>	bmpr2a-3303	CAGAGTGAGCAGAGGGAGTGT		
	bmpr2a-3304	CAGCGGTGTCCTTGATAACAG		
<i>bmpr2b</i>	bmpr2b-3347	GAATCCATCCAGAAGCGGCA		
	bmpr2b-3348	GGGGTATATTTACCGGCCACA		
<i>fshb</i>	fshb_176	CAGATGAGGATGCGTGTGC		Real-time qPCR
	fshb_177	ACCCCTGCAGGACAGCC		
<i>cyp19a1a</i>	cyp19a1a_818	TGTGCGTGTCTGGATCAATGG		
	cyp19a1a_819	AAGCCCTGGACCTGTGAGAG		
<i>inhbaa</i>	inhbaa-931	AACAGGCAGAACAGACGGAGATC		
	inhbaa-932	GCAGCCGAATGTTGACGTTAGC		
<i>efla</i>	efla_728	GGCTGACTGTGCTGTGCTGATTG		
	efla_729	CTTGTCGGTGGGACGGCTAGG		